Treatment of the Results of Magnetic Mapping of the SIBERIA-2 Magnets

V.Korchuganov, E.Levichev, and A.Philipchenko
Budker Institute of Nuclear Physics
630090 Novosibirsk, Russia

Abstract

Recently the fabrication and the assembling of all the main magnetic elements for a 2.5 GeV dedicated SR source SIBERIA-2 have been completed. The paper reports a technique for high accurate measuring the field of different types of magnets. The measurement results have been treated statistically and an effective mechanism to correct the magnetic length of the dipoles and quadrupoles has been developed.

I. INTRODUCTION

The 2.5 GeV SIBERIA-2 storage ring is a dedicated SR source. It has optimized low-emittance lattice with six-fold symmetry [1] which contains 24 zero-gradient dipoles, 72 quadrupoles of three different lengths, 36 sextupoles and 12 octupoles. The design of the magnets was presented in ref. [2]. All the magnets except the quadrupoles were built and installed at the ring. The manufacture of quadrupoles will be completed in the near future. All the magnets were involved in series magnetic measurements. The test procedure and the treatment of the magnetic mapping results are described in this report.

II. HALL PLATES MEASUREMENT

A familiar Hall probes technique was chosen for magnetic tests. To make point-by-point measurements of the magnetic field the Hall plate bench system for VEPP machines [3] supplied by Karl Zeiss Jena was used. The mechanical positional accuracy along the magnet axis is 6 μm. The single pass scan length available is 0.8 m. To extend the scan length it is possible to shift the initial scanning coordinate without any accuracy reduction. The Hall probes, which have low temperature coefficient ($5 \times 10^{-5}/°C$) do not need special control over the probes temperature. A set of probes was glued on the support, and the distance between adjacent probes was measured at an accuracy better than 6 μm. A sufficiently high output ($10\mu V/Gauss$) makes it possible to read the signal directly with the digital voltmeter. A special constant current source was built for the measurements with the relative current variation $\leq 10^{-4}$.
Prior to the measurement Hall probes were calibrated against a high precision NMR probe [4] using a dipole magnet with a high uniform field. The calibration curves were fitted by a spline interpolation technique in the range of ± 2.2 T.
All the electronics involved was produced in CAMAC standard. The data were read by a microcomputer. The software for analyzing, plotting and storing the measurement results was developed.
The Hall plates array is transversal aligned in the magnet gap with the precision ≤ 0.2 mm using the alignment marks.

III. DIPOLE MAGNETS

The main characteristics of the dipole are given in Table 1. The specific feature of the H-shaped solid Armco-steel magnet is its "soft-end" which is a constant field region with the field equal to one quarter of the main field to produce softer radiation [2]. For symmetry this soft-end pole must be alternatively at the left or at the right end of magnets, thus creating two separate families.

Table 1. Dipole design parameters

	Main pole	Soft-end pole
Bend angle	14.33°	0.67°
Field (2.5 GeV)	1.7 T	0.425 T
Bending radius	4905.4 mm	19622 mm
Magnetic length	1227 mm	230 mm
Gap	42 mm	42 mm
Turns per pole	4	1

Point-by-point measurements have been carried out with an array of 11 Hall probes with 18 mm spacing. Table 2 lists the results of the excitation curve measurements for the central part of the main pole. The optimized yoke geometry has permitted us to reach the nonlinearity of the excitation curve $\leq 3\%$ at 2.5 GeV.

0-7803-1203-1/93$03.00 © 1993 IEEE

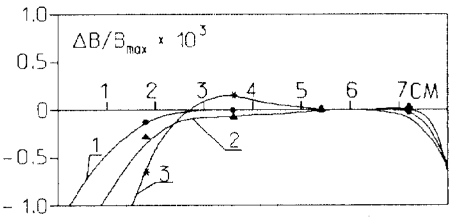

Figure 1: Dipole magnet field uniformity. 1 - 6.5 kA, 2 - 8.5 kA and 3 - 10.5 kA

Table 2. Field versus current for the dipole main pole

I (kA)	1	2	3	4	5
B (T)	.24	.47	.72	.95	1.19
I (kA)	6	7	8	9	10.5
B (T)	1.41	1.64	1.82	1.95	2.17

Fig. 1 shows the field homogeneity at the center of the dipole at several excitation levels. Despite the operation current is 7.3 kA (1.7 and 2.5 GeV), the measurement results demonstrate rather good field quality at 10.5 kA (2.17 T and 3.2 GeV). The field deviation is within the limit $\pm 5 \times 10^{-4}$ in the region ± 3.1 cm at the excitation level 7.5 kA and is within the limit $\pm 5 \times 10^{-4}$ in the region ± 2.8 cm at the excitation level 10.5 kA. One can see that saturation effects do not seriously degrade the field quality. Due to the large pole width (260 mm) in radial direction the horizontal distribution of the field integral in the working aperture is practically the same as the field profile.

Field mapping was performed directly through the magnet with a 1 cm point spacing. After that, the field profile was calculated using spline interpolation near the electron trajectory which was previously found. The field profile along the electron trajectory is given in Fig. 2. To use

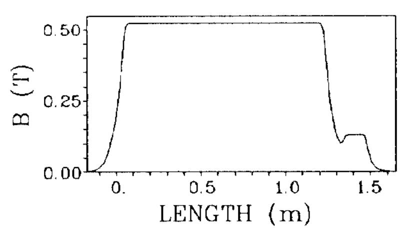

Figure 2: Longitudinal profile of the dipole field.

a hard-edge approximation, the proper ratio between the main and soft-end pole field integrals in the intersection region should be taken into account. Calculations with MERMAID [5] have been done and the integral ratio coefficient was found [6]. The effective length for the appropriate part of the dipole was determined as the ratio of the field integral of this part to the central field amplitude. Unlike the previously used model, a three sectionized magnet (main pole region, zero field region, and soft-end region) has proved to be more convenient. According to the measurement results, the effective lengths variation in the working field interval does not exceed $\pm 0.05\%$. The mean effective lengths and their rms deviations over all the SIBERIA-2 dipoles are presented in Table 3.

Table 3. Dipole effective lengths parameters.

	Main pole section	Zero-field section	Soft-end section
l (m)	1.2422 m	0.052 m	0.175 m
σ_l	1.196 mm	0.397 mm	0.416 mm
σ_l/l	9.6×10^{-4}	7.6×10^{-3}	2.4×10^{-3}

Fig. 3 presents the relative deviation of the bend angle of individual dipoles with respect to its average value over all the magnets.

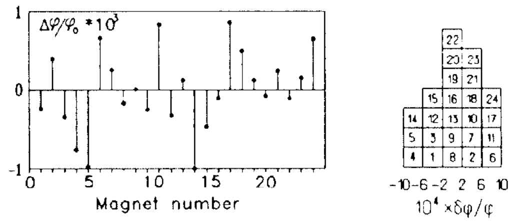

Figure 3: Relative deviation of the bend angle of dipoles with respect to its average value over all the magnets.

IV. Quadrupole magnets

Three types (A, B and C) of quarupole magnets differing by their yoke length constitute 6 families [2]. The main parameters of quadrupoles are summarized in Table 4.

Table 4. Main parameters of SIBERIA-2 quadrupoles at 2.5 GeV

Type	A	B	C
Bore radius	28 mm	28 mm	28 mm
Max. gradient	30 T/m	36 T/m	30.5 T/m
Steel length	26.4 cm	36.2 cm	28.8 cm
Turns per pole	15	15	14
Max. current	0.66 kA	0.81 kA	0.67 kA

All the quadrupoles are made of solid Armco-steel. $A-$ and $B-$types quadrupoles are of the conventional "close-side" design, while the yoke of the $C-$ type quadrupole is split into two symmetric halves - top and bottom - to pass the SR beam lines, without steel connections between them. The halves are joined through strong aluminum spacers.

The pole profile is shaped as $y = 392/x$ hyperbola which is ended by 5-mm-wide strips at $x = 42.15$ mm. The good gradient region is formed by the pole profile without shimming being inefficient in our case, because the shimms iron

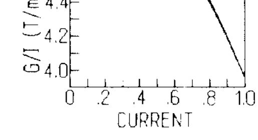

Figure 4: SIBERIA-2 quadrupole excitation curve.

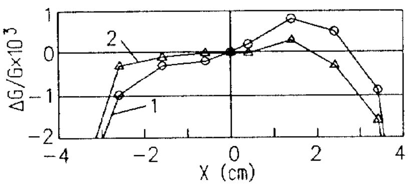

Figure 5: The quadrupole gradient uniformity. 1 - 0.75 kA and 2 - 0.50 kA

is saturated due to the high magnetic field.
The excitation curve measurement results are demonstrated in Fig. 4.
The measurements were performed with a set of 11 Hall probes of 6 mm spacing at several excitation current levels. The set of probes was located horizontally (in the mid plane) and vertically (normal to the mid plane) in the lens aperture, and the field was mapped point-by-point with a 0.5-cm spacing in longitudinal direction.
In Fig. 5 the gradient uniformity for different current levels in the A – quadrupole center is shown. The quadrupoles edge fields have a considerable effect on the integrated gradient uniformity, and special studies have been carried out to find optimal pole chamfer sizes. Fig. 6 shows the integrated gradient homogeneity for several chamfer sizes. The 6 mm × 45° chamfer was chosen on the basis of the results

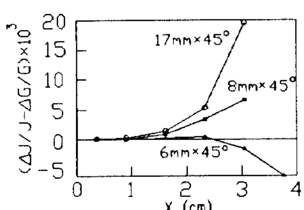

Figure 6: The contribution of the edge field to the integrated gradient homogeneity for several chamfer sizes.

obtained. Fig. 7 demonstrates the integrated gradient homogeneity of the same A – quadrupole at two excitation levels. The good integrated gradient region (within the specified limits $\pm 5 \times 10^{-4}$) lies within ±2.2 cm.
In Table 5 the characteristics which demonstrate the effect of saturation on the quadrupole parameters are listed. $(\int G(s)ds)/G_0$ determines the dependence of the on-axis effective length on the exitation current, whereas $(\int G(s)ds)/I$ also incorporates the yoke saturation caused by the transverse magnetic flux. Here G_0 is the gradient

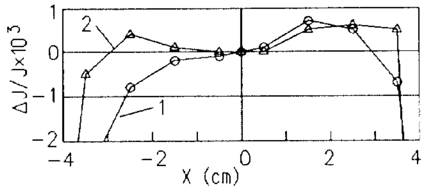

Figure 7: The integrated gradient homogeneity at several excitation levels. 1 - 0.75 kA and 2 - 0.5 kA

in the quadrupole centre and I is the excitation current.

Table 5. Quadrupole saturation effects characteristics

I (kA)	$\int G(s)ds$ (T)	G_0 (T/m)	$\int G(s)ds/I$ (T/kA)	$\int G(s)ds/G_0$ (m)
0.75	9.9010	33.951	13.20	0.291
0.50	6.9697	23.805	13.94	0.293
0.25	3.5046	11.965	14.02	0.293

V. Acknowledgement

The contribution of S.Mikhailov to the development of the measurement system and software for treating the results as well as for performing magnets measurements are gratefully acknowledged.

References

[1] V.Anashin, A.Valentinov et al, "The dedicated SR source SIBERIA-2", The proceedings of the 11-th Russian Particle Conference, Dubna 1989, p.277-280 (in Russian).

[2] G.I.Erg et al, "Magnetic lattice of SIBERIA-2 - dedicated SR source", Preprint INP 89-174, Novosibirsk 1989.

[3] P.Vobly et al, "The VEPP magnetic measurements", The Proceedings of the 3-th USSR Particle Conference, Moscow 1973, vol.2, p.87-90 (in Russian).

[4] N.Zinevitch et al, "NMR field measurement system", The proceedings of the 10-th USSR Particle Conference, Dubna 1986, vol.1, p.342-347 (in Russian).

[5] A.Dubrovin, "MERMAID Reference Manual, INP Internal Report, Novosibirsk 1992.

[6] S.Mikhailov, private communication